ARTIFICIAL IMMUNE NETWORK-BASED MULTI-ROBOT FORMATION PATH PLANNING WITH OBSTACLE AVOIDANCE

Lixia Deng,* Xin Ma,* Jason Gu,*,** Yibin Li,* Zhigang Xu*** and Yafang Wang****

Abstract

Artificial immune network algorithm (AINA) combined with position tracking control method is used for multi-robot formation path planning. The proposed algorithm avoids obstacles and recovers formation for follower robot after passing around obstacles. Different methods are adopted to calculate the steering direction and the linear velocity of the follower robot. Steering direction of the follower robot is computed with AINA. AINA has abilities of self-recognition and diversity, and solves the problems of local minima and immature convergence. The optimal steering direction selected with AINA quickly tends towards the steering direction of leader robot, and successfully avoids obstacles. The linear velocity of follower robot is computed with position tracking control method. It is computed based on the state of leader robot, current position of follower robot, and position of virtual robot. It guarantees that the position errors of follower robot quickly converge to zeros. The asymptotic stability of the entire formation system is proven with Lyapunov theory. Numerous experiments validate that the proposed algorithm successfully avoids obstacles and quickly tracks the leader robot for follower robot.

Key Words

Artificial immune network algorithm, position tracking control method, multi-robot formation, obstacle avoidance

1. Introduction

Formation control [1]–[3] is a typical problem for multi-robot systems. Multi-robot formation is defined as the coordination of robots in a group to get into and to maintain a formation with a certain shape, and it should adapt to the constraints of environments. The main difficulty in multi-robot formation is how to maintain a pose for each robot depending on the poses of other robots in order to reach a desired goal.

Leader–follower method [4]–[6] is widely used for multi-robot formation. Follower robots track the leader robot with the desired distance separation and bearing angle. Stable tracking control method is widely used for the follower robot tracking the leader robot. The aim of stable tracking controller is to have the follower robot follow a reference trajectory and to have the tracking error converge to zero.

Yang *et al.* [7] maintained the formation using the error tracking system model which was derived based on the-off-axis point of the follower tracking the-off-axis point on the virtual robot. The zero dynamics stability of the system is guaranteed with the constraint of the initial orientation. Chetty *et al.* [8] proposed a closed-loop tracking controller and utilized the behaviour-based reactive controller to form the formation and navigate robots. The exchange of leadership is incorporated in the system to avoid obstacles in the follower path, but it raises the deadlocks between the robots. Dai and Lee [9] proposed a leader-waypoint-follower formation controller based on relative motion states of mobile robots. Stable tracking control method combines receding horizon (RH) tracking control method to form and maintain the formation. But, the combined algorithm cannot achieve formation with obstacle avoidance.

Formation with obstacle avoidance for follower robot is a challenge for multi-robot formation systems. Follower robot cannot navigate itself if detecting obstacles, because follower robot needs not only to avoid obstacles, but also to recover the formation after passing around obstacles.

Yang *et al.* [10] proposed two control algorithms based on suboptimal model predictive control for formation control and obstacle avoidance. Zhang *et al.* [11] utilized artificial potential field algorithm to avoid obstacles for

* School of Control Science and Engineering, Shandong University, Jinan, Shandong, China; e-mail: amanda19881119@gmail.com, {maxin, liyb}@sdu.edu.cn

** Department of Electrical and Computer Engineering, Dalhousie University, Halifax, Nova Scotia, Canada; e-mail: Jason.gu@dal.ca

*** Institute of Developmental Biology, School of Life Sciences, Shandong University, Jinan, Shandong 250100, P. R. China; e-mail: xuzg@sdu.edu.cn

**** School of Computer Science and Technology, Shandong University, Jinan, Shandong, China; e-mail: yafang.wang@sdu.edu.cn

Recommended by Prof. Howard Li
(DOI: 10.2316/Journal.206.2016.3.206-4746)

leader–follower formation in unknown environments. Gomez *et al.* [12] used the Fast Marching Square method with no local minima problem for leader–follower formation with obstacle avoidance. Liu *et al.* [13] developed an improved rapidly exploring random tree to plan the path for each robot and developed a dynamic priority strategy to solve the conflicts caused by orders of robots in forming the formation. Dai and Lee [14] proposed a geometric obstacle avoidance control method to guarantee that the robot avoided the static and dynamic obstacles using onboard sensors.

Artificial immune algorithm with abilities of self-recognition, adaptation, and self-learning is widely used for multi-robot path planning. Luh and Liu [15] proposed a reactive immune network for mobile robot navigation in unknown environments. Adaptive virtual target method is integrated to solve the problem of local minima. But it has an immature convergence problem. Deng *et al.* [16] proposed a poly-clonal-based artificial immune network algorithm (AINA) for path planning with obstacle avoidance in complex environments. Immunity poly-clonal algorithm is integrated to solve the problems of immature convergence and local minima. Deng *et al.* [17] proposed an improved poly-clonal artificial immune algorithm for multi-robot formation with obstacle avoidance. Leader-change is utilized for follower robot avoiding obstacles. Follower robot reaches the desired virtual position and leader robot reaches the goal with improved poly-clonal artificial immune algorithm. Deng *et al.* [18] proposed a dynamic formation path planning algorithm combining leader–follower method and improved poly-clonal artificial immune algorithm. Formation-change and leader-change are used for obstacle avoidance. But in [17], [18], leader robot needs to wait for the follower robot forming the formation.

Contributions of this paper lie in the following perspectives. (1) The proposed algorithm combining AINA and position tracking control method is used for multi-robot formation path planning with obstacle avoidance. To simplify the problem, we consider from different views and adopt different methods to calculate the steering direction and the linear velocity of the follower robot. (2) Steering direction of the follower robot is calculated with AINA which solves the problems of local minima and immature convergence. It is influenced by the steering direction of leader robot, the azimuth of virtual robot, and distance from obstacle. The optimal steering direction quickly tracks the steering direction of leader robot, and successfully avoids obstacles. (3) Linear velocity of the follower robot is calculated with position tracking control method without the constraints of angular velocity and the initial orientation. It guarantees the follower robot tracking leader robot forming the formation quickly. Lyapunov theory is used to prove the system stability.

The remainder of the paper is organized as follows. Section 2 describes the formation model. The computation of steering direction with AINA is discussed in Section 3. Section 4 presents the computation of linear velocity for follower robot with position tracking control method. Section 5 describes the experimental results along with some discussions. Section 6 describes several experiments in MobileSim simulator. Finally, Section 7 concludes the paper.

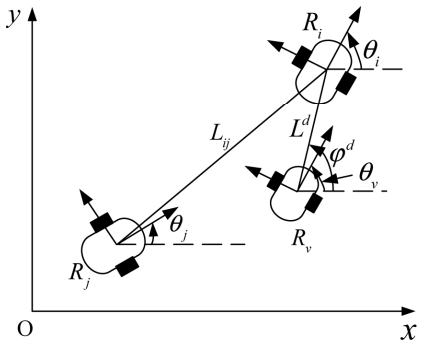

Figure 1. Leader–follower formation model.

2. Formation Model

The posture of each robot is described in terms of $[x \quad y \quad \theta]^T$, where x, y represent the x and y coordinates, and θ represents the orientation of robot. The kinematics model of a mobile robot is:

$$\begin{bmatrix} \dot{x} \\ \dot{y} \\ \dot{\theta} \end{bmatrix} = \begin{bmatrix} \cos\theta & 0 \\ \sin\theta & 0 \\ 0 & 1 \end{bmatrix} \begin{bmatrix} v \\ \omega \end{bmatrix} \tag{1}$$

Where v is the linear velocity and ω is the angular velocity of the robot.

The model of leader–follower formation system is shown in Fig. 1. Postures of the leader robot R_i, the follower robot R_j, and the virtual robot of follower robot R_v are described in terms of $[x_o \quad y_o \quad \theta_o]^T$, $o = i, j, v$. L^d, φ^d represent the desired separation distance and bearing angle between R_i and R_v. L_{ij}, φ_{ij} represent the actual separation distance and bearing angle between R_i and R_j.

Positions of the virtual robot and the follower robot are calculated based on Fig. 1:

$$\begin{bmatrix} x_v \\ y_v \end{bmatrix} = \begin{bmatrix} x_i \\ y_i \end{bmatrix} - L^d \begin{bmatrix} \cos\varphi^d \\ \sin\varphi^d \end{bmatrix} \tag{2}$$

$$\begin{bmatrix} x_j \\ y_j \end{bmatrix} = \begin{bmatrix} x_i \\ y_i \end{bmatrix} - L_{ij} \begin{bmatrix} \cos\varphi_{ij} \\ \sin\varphi_{ij} \end{bmatrix} \tag{3}$$

In this paper, leader robot reaches the goal with obstacle avoidance and follower robot quickly tracks the leader robot with obstacle avoidance. Steering direction of follower robot is computed with AINA and the linear velocity of follower robot is computed with position tracking control method.

3. Artificial Immune Network Algorithm

Artificial immune algorithm increases the diversity of antibodies, and solves the problems of immature convergence and local minima [19]. The steering direction of follower robot is computed with AINA. Follower robot with the optimal steering direction moves towards virtual robot and avoids obstacles. Meanwhile, leader robot utilizes AINA for path planning with obstacle avoidance. The adjacent robot within the detection radius is considered as an obstacle.

3.1 Artificial Immune Network Algorithm for Follower Robot

AINA defines an antigen and antibody based on the environmental information and postures of robots. Based on the interaction between antigen and antibody and the interaction between antibodies, AINA selects the antibody with the highest concentration as the final antibody; *i.e.*, based on the interaction between robot and environment, AINA selects the steering direction with the highest possible as the final steering direction.

Antigen set of the follower robot detected by sensors (sonars) mainly provides environmental information. It includes the steering direction of leader robot θ_i, the azimuth of virtual robot θ_{gv}, the distance between obstacle and f-th sensor of follower robot d_f, and the azimuth of f-th sensor θ_{S_f}. Antibody represents the steering direction of follower robot. Antibody set Ab is defined based on $Ab_s \equiv \theta_s = 2\pi(s-1)/N_{Ab},\ s = 1, 2, \ldots, N_{Ab}$, where Ab_s represents the s-th antibody, N_{Ab} represents the number of antibodies, and θ_s represents the s-th possible steering direction (s-th antibody).

The concentration of each antibody is calculated based on (4) and (5) [15]–[17]:

$$\frac{dA_s(t)}{dt} = \left(\sum_{s_1=1}^{N_{Ab}} \cos(\theta_s - \theta_{s_1})\, a_{s_1}(t) + m_s - k_s \right) a_s(t) \quad (4)$$

$$a_s(t) = \frac{1}{1 + \exp(0.5 - A_s(t))} \quad (5)$$

where $s, s_1 = 1, 2, \ldots, N_{Ab}$ represents subscripts to distinguish the antibody types, a_s represents the concentration of s-th antibody, dA_s/dt denotes the rate of change of concentration; (4) is composed of three terms. The first term indicates the stimulative-suppressive affinity between antibodies. The second term depicts the stimulus from antigen, and m_s represents the affinity between antigen and s-th antibody. The final term depicts the natural extinction term which indicates the dissipation tendency in the absence of any interaction, and k_s represents the natural death coefficient, $k_s = 0.5$, (5) depicts a squashing function to ensure the stability of the concentration.

m_s for the follower robot is calculated based on its antigen set; m_s is calculated with (6):

$$m_s = \tau_1 F_{goal_1} + \tau_2 F_{goal_2} + \tau_3 F_{obs} \quad (6)$$

where τ_1, τ_2, τ_3 are positive constants, and $\tau_1 + \tau_2 + \tau_3 = 1.0$. F_{goal_1} represents the attraction of s-th antibody from leader robot, F_{goal_2} represents the attraction of s-th antibody from virtual robot, and F_{obs} represents the repulsion of s-th antibody from obstacles.

$F_{goal_1}, F_{goal_2}, F_{obs}$ are calculated with (7)–(9):

$$F_{goal_1} = \frac{1.0 + \cos(\theta_s - \theta_i)}{2.0} \quad (7)$$

$$F_{goal_2} = \frac{1.0 + \cos(\theta_s - \theta_{gv})}{2.0} \quad (8)$$

$$F_{obs} = \sum_{f=1}^{N_S} \exp^{N_{Ab}} \cdot \bar{d}_f \cdot \frac{1.0 + \cos\left(\theta_s - \theta_{S_f}\right)}{2.0} \quad (9)$$

where $s = 1, 2, \ldots, N_{Ab},\ 0 \le F_{goal_1} \le 1,\ 0 \le F_{goal_2} \le 1,\ N_S$ is the number of sensors, $\bar{d}_f$ represents the normalized distance between obstacle and f-th sensor.

Based on m_s, the concentration of each antibody can be calculated. To solve the local minima problem and immature convergence problem, concentration of each antibody needs to be recalculated based on Algorithm 1 [17].

Algorithm 1. The optimal antibody selection.

Require: Concentration of each antibody
Ensure: The optimal antibody

Clonal operator
Concentration is divided into q_c same concentrations (initial population), and q_c is calculated based on the affinity between antigen and antibody.

Crossover operator
It chooses an intersection from two antibodies and exchanges one or some components of two antibodies.

Mutation operator
It changes some genes in the population and the exchange negates some genetic value, *i.e.*, 0→1 or 1→0.

Selection operator
The antibody with the highest concentration is selected as the optimal antibody.

Algorithm 1 adopts four operators to select the optimal antibody. It utilizes crossover operator to exchange information between antibodies and utilizes mutation operator to increase the diversity of antibody. Algorithm 1 increases the diversity of antibody and overcomes the problems of local minima and immature convergence.

The antibody with the highest concentration is selected as the optimal antibody. The optimal antibody corresponds to a steering direction of follower robot. Follower robot moves with the steering direction which quickly tends towards the steering direction of leader robot and successfully avoids obstacles.

3.2 Artificial Immune Network Algorithm for Leader Robot

AINA is used for the leader robot path planning with obstacle avoidance. In the path planning, linear velocity of the leader robot is a constant.

Antigen set of leader robot detected by sensors includes the azimuth of goal θ_g, the distance between obstacle and f-th sensor of leader robot d_f, and the azimuth of sensor θ_{S_f}. Antibody represents the steering direction of leader robot. The concentration of each antibody is computed with (4) and (5).

The affinity between antigen and s-th antibody m_s for leader robot is computed with (10):

$$m_s = \mu_1 F_{goal} + \mu_2 F_{obs} \tag{10}$$

where μ_1, μ_2 are positive constants, and $\mu_1 + \mu_2 = 1.0$. F_{goal} represents the attraction of s-th antibody from goal, and $F_{goal} = (1.0 + \cos(\theta_s - \theta_g))/2.0$, where $0 \le F_{goal} \le 1$. F_{obs} calculated with (9) represents the repulsion of s-th antibody from obstacle.

To solve the problems of local minima and immature convergence, concentration of each antibody is recalculated by Algorithm 1. The antibody with the highest concentration is selected as the optimal antibody, and its corresponding steering direction acts on leader robot.

Steering direction of the follower robot is calculated with AINA. Follower robot with the optimal steering direction quickly tends towards the steering direction of leader robot, and successfully avoids obstacles. Moreover, leader robot plans for the path with obstacle avoidance using AINA.

4. Position Tracking Control Method

Position tracking control method calculates the linear velocity of follower robot v_j.

4.1 Tracking Algorithm

The linear velocity of follower robot is calculated with position tracking algorithm. Position error between the actual position and virtual position of follower robot is calculated based on (11):

$$E = \begin{bmatrix} e_x \\ e_y \end{bmatrix} = \begin{bmatrix} \cos\theta_j & \sin\theta_j \\ -\sin\theta_j & \cos\theta_j \end{bmatrix} \begin{bmatrix} x_v - x_j \\ y_v - y_j \end{bmatrix} \tag{11}$$

The derivative matrix $\dot{E}$ can be derived as (12):

$$\dot{E} = \begin{bmatrix} \dot{e}_x \\ \dot{e}_y \end{bmatrix} = \begin{bmatrix} \cos(\theta_i - \theta_j) \\ -\cos(\theta_i - \theta_j) \end{bmatrix} v_i + \begin{bmatrix} -1 \\ 1 \end{bmatrix} v_j \tag{12}$$

Based on the position error between actual position and virtual position of follower robot, the linear velocity of follower robot is considered as (13):

$$v_j = v_i \cos(\theta_i - \theta_j) + K_1 e_x - K_2 e_y \tag{13}$$

where K_1, K_2 are positive constants. v_j is bounded for all t, and $v_j \le \min\left\{V_{\max}, \left(\sqrt{(x_v - x_j)^2 + (y_v - y_j)^2}\right)/t\right\}$.

4.2 Stability Analysis

Lyapunov theory proves that the tracking system with linear velocity of follower robot (13) is asymptotically stable and its asymptotically stable equilibrium point is $E = 0$.

Proposition 1. *Assuming that the linear velocity of follower robot is calculated with (13), $v_i > 0, e_x \in R, e_y \in R$, then as $t \to \infty, E = 0$ is an asymptotically stable equilibrium point.*

Proof: Lyapunov function is selected as $V(E) = 0.5K_1 e_x^2 + 0.5K_2 e_y^2$, where $V(E) \ge 0$, and $V(E) = 0$ if and only if $e_x = 0$, $e_y = 0$. K_1 and K_2 are positive constants.

The derivative of Lyapunov function is given by $\dot{V}(E) = K_1 e_x \dot{e}_x + K_2 e_y \dot{e}_y$.

Substituting (11)–(13) into the derivative of Lyapunov function $\dot{V}(E)$ gets $\dot{V}(E) = K_1 e_x (\cos(\theta_i - \theta_j) v_i - v_j) + K_2 e_y (-\cos(\theta_i - \theta_j) v_i + v_j) = -(K_1 e_x - K_2 e_y)^2 \le 0$.

So the tracking system under the control input (13) is asymptotically stable.

Based on the Barbalat's lemma [9], [20], $V(E) = 0.5K_1 e_x^2 + 0.5K_2 e_y^2 \ge 0$, it has a lower bound, $\dot{V}(E) = -(K_1 e_x - K_2 e_y)^2 \le 0$ is a negative definite function and it is uniformly continuous about time t, so $\lim_{t\to\infty} \dot{V}(E) = 0$, *i.e.*, $\lim_{t\to\infty} -(K_1 e_x - K_2 e_y)^2 = 0$, so $\lim_{t\to\infty} e_x = 0$, $\lim_{t\to\infty} e_y = 0$. ■

So the proposed linear velocity for follower robot guarantees the stability of tracking system and its asymptotically stable equilibrium point is $E = 0$.

Steering direction of follower robot is calculated with AINA, and the linear velocity of follower robot is calculated with position tracking control method. The combination algorithm ensures that follower robot quickly follows the leader robot and successfully avoids obstacles.

5. Experiments and Discussions

To validate the proposed algorithm, several simulations are performed with Matlab. Each robot is regarded as a sphere, and it moves towards an arbitrary direction in $[0, 2\pi]$. Leader robot's velocity is specified as $v_i = 0.1\,\mathrm{m/s}$. In this paper $\tau_1 = 0.4$, $\tau_2 = 0.5$, $\tau_3 = 0.1$, $\mu_1 = \mu_2 = 0.5$, $V_{\max} = 0.5\,\mathrm{m/s}$, $K_1 = 0.3\,\mathrm{s}^{-1}$, and $K_2 = 0.08\,\mathrm{s}^{-1}$.

5.1 Formation Switching

The simulation is utilized to validate that the proposed algorithm successfully achieves formation switching. The comparison with the stable tracking control method combining with RH tracking control method [9] validates the superiority of the proposed algorithm.

Figure 2(a) shows the formation path planning trajectories where three robots switch from an equilateral

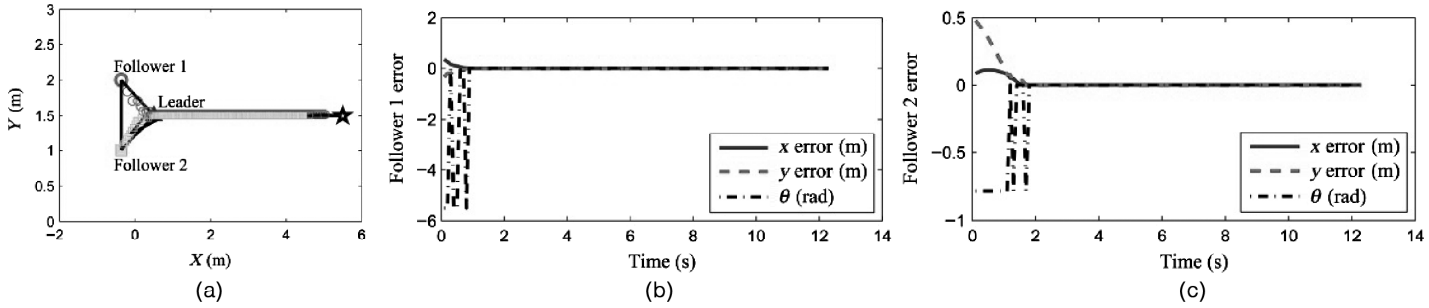

Figure 2. Formation switching with the proposed algorithm: (a) trajectories; (b) state errors of follower 1; and (c) state errors of follower 2.

Table 1
Comparison of Error Convergence Times with Different Algorithms

The Proposed Algorithm	Error Convergence Time (s)			
	Follower robot 1	x	y	θ
		1.6	1.4	1.5
	Follower robot 2	x	y	θ
		1.8	1.7	1.7
Algorithm in [9]	Error Convergence Time (s)			
	Follower robot 1	x	y	θ
		5.4	4.5	4.5
	Follower robot 2	x	y	θ
		1.5	1.5	1.5

triangle to a line. Initial positions of leader robot, follower robots 1 and 2 are specified as (0.5, 1.5) m, $((0.5-\sqrt{0.75}), 2)$ m, and $((0.5-\sqrt{0.75}), 1)$ m. The desired distance and desired bearing angle between two robots are $L^d = 0.4$ m and $\varphi^d = 0$, respectively.

Figure 2(b) and 2(c) show the state errors of two follower robots in the process of formation switching. We note that follower's state errors converge to zeros correctly and efficiently.

State error convergence times of two follower robots with different algorithms are shown in Table 1. The table explains that the convergence time with the proposed algorithm is less than the algorithm in [9]. Follower robot 2 has the resultant force from virtual robot and leader robot in opening environment and it is far away from leader robot, the attraction from leader robot is smaller than follower robot 1, so its convergence time is longer than follower robot 1. Meanwhile, stable state errors of two follower robots achieve $10^{-5}\,m$ in the multi-robot formation path planning.

With the proposed algorithm, multi-robot systems quickly form the desired formation and state errors of the system correctly converge to zeros. Its performance is better than the method in [9].

5.2 Formation with Obstacle Avoidance

The simulation is used to validate that the proposed formation path planning algorithm successfully forms the desired formation with obstacle avoidance. The comparison with [18] validates effectiveness of the proposed algorithm.

Figure 3 shows several results of formation path planning with obstacle avoidance. Initial positions of leader robot, and two follower robots are specified as (4,6) m, (1,5) m, and (10,2) m. The position of the goal is specified as (15,15) m. Positions of obstacles are specified as (8,2) m and (9,10) m. Size of the obstacle is specified as 0.5 m × 0.5 m. The desired formation shape is an equilateral triangle, and the desired distance is $L^d = 3$ m.

Figure 3(a) indicates the formation path planning trajectories with obstacle avoidance. Obstacles are on trajectories of follower robot 2 and leader robot. We note that follower robot 2 successfully avoids the obstacle and tracks leader robot with the desired distance and angle.

Figure 3(b)–3(e) indicate the position errors of two follower robots in the process of formation path planning with the proposed algorithm and the algorithm in [18]. Figure 3(f) indicates the distances between robots and obstacles. We note that robots successfully avoid obstacles in the formation path planning.

Table 2 shows the position error convergence times of two follower robots with different algorithms.

In Figure 3(b)–3(e) and Table 2, we note that x errors and y errors convergence times with the proposed algorithm are much smaller than the algorithm in [18]. With the algorithm in [18], the system changes the formation from a triangle to a line, and position errors of two follower robots do not completely converge to zeros when the leader robot encounters the obstacle. The proposed algorithm does not need to change formation when robots encounter obstacles, and it can preferably keep and form formation. With the proposed algorithm, follower robot 2 quickly forms the formation and avoids the obstacle, and two follower robots successfully keep the formation when the leader robot avoids the obstacle.

With the proposed algorithm, multi-robot systems successfully avoid obstacles with the desired formation, and follower robots quickly track leader robot with obstacle avoidance.

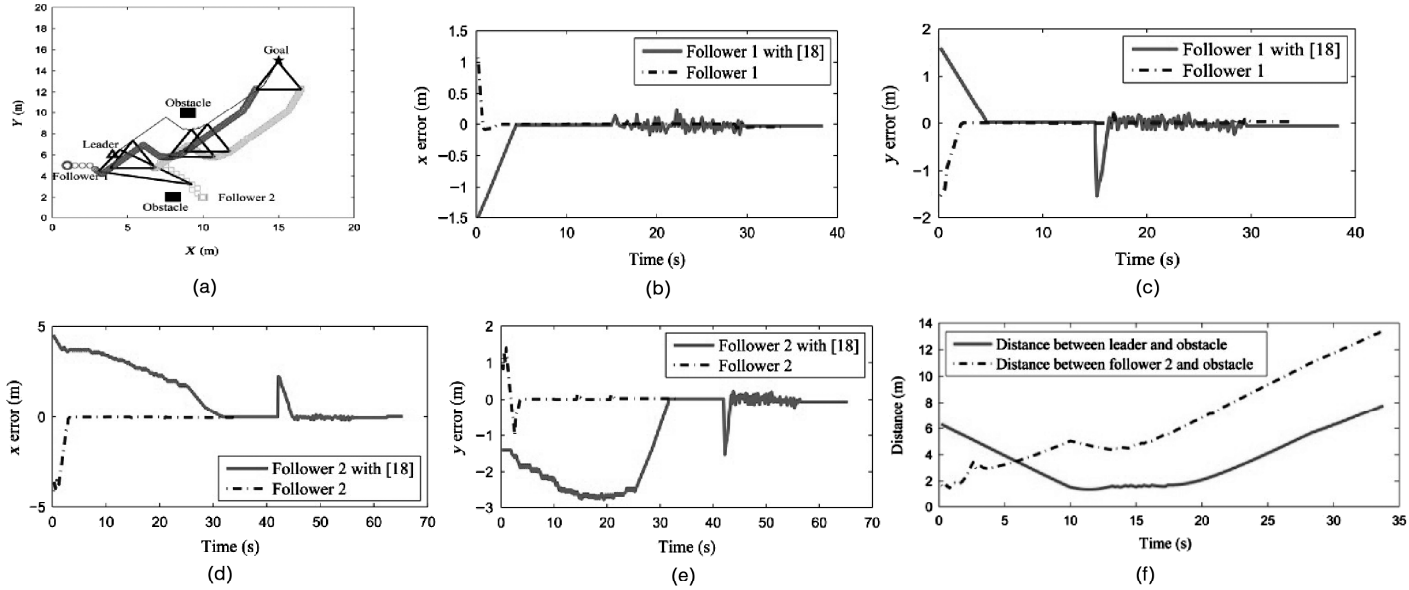

Figure 3. Formation path planning with obstacle avoidance using different algorithms: (a) trajectories; (b) x errors of follower 1; (c) y errors of follower 1; (d) x errors of follower 2; (e) y errors of follower 2; and (f) distances between robots and obstacle.

Table 2
Comparison of Error Convergence Times with Different Algorithms

The Proposed Algorithm	Error Convergence Time (s)		
	Follower robot 1	x	y
		2.4	2.4
	Follower robot 2	x	y
		3.8	3.8
Algorithm in [18]	Error Convergence Time (s)		
	Follower robot 1	x	y
		4.4	4.4
	Follower robot 2	x	y
		31.4	31.4

5.3 Formation Forming and Keeping

The simulation is used to validate that the proposed algorithm quickly forms the formation and the system successfully reaches the goal with the desired formation. The comparison with [17] validates the effectiveness of the proposed algorithm.

Figure 4 shows several simulation results where four robots form the desired formation and keep formation in the process of reaching the goal. Initial positions of leader robot, three follower robots are specified as (6,7) m, (1,6) m, (10,2) m, and (3,3) m. The position of goal is specified as (15,13) m. The desired formation shape is a diamond. The desired distance between any two robots is $L^d = 3$ m. The time step equals 0.2 s.

Figure 4(a) shows the formation trajectories. Three follower robots quickly form the formation and achieve path planning with the desired formation.

Figure 4(b) and 4(c) show the position errors of three follower robots in the formation path planning. We note that the position errors of three follower robots quickly converge to zeros, and four robots successfully reach the goal with the desired formation.

The position error convergence times of three follower robots are given in Table 3. The table explains that the error convergence time of the proposed algorithm is much less than the algorithm in [17]. Meanwhile, the time of reaching goal with the proposed algorithm is much less than the algorithm in [17], because leader robot does not need to wait for the follower robot forming the formation.

The proposed algorithm not only quickly forms the formation, but in real-time tracks leader robot in multi-robot formation path planning.

6. MobileSim Experiments

The experiments validate the proposed algorithm in MobileSim simulator. The simulator is a connection option that provides a virtual replacement for AmigoBot. It has eight sonars used for object detection and distance detection. The program performing on the simulator has the same effect with the program performing on the actual robot's PC.

In the experiment, three robots are placed with the initial configurations of (0,0) m, (0, −1) m, and (0, −2) m. Linear velocity of leader robot is specified as $v_i = 0.15$ m/s, and the maximum linear velocity of follower robot is specified as $V_{\max} = 0.5$ m/s.

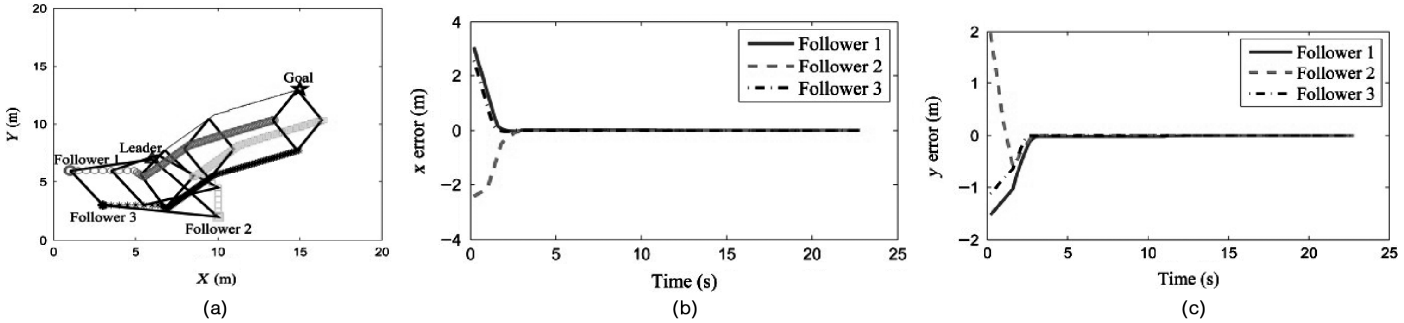

Figure 4. Formation with the proposed algorithm: (a) trajectories; (b) x errors of three followers; and (c) y errors of three followers.

Table 3
Comparison of Error Convergence Times with Different Algorithms

The Proposed Algorithm	Error Convergence Time (s)			Time of Reaching Goal (s)
	Follower robot 1	x	y	22.8
		3.0	3.0	
	Follower robot 2	x	y	
		3.0	2.8	
	Follower robot 3	x	y	
		2.6	2.6	
Algorithm in [17]	Error Convergence Time (s)			Time of Reaching Goal (s)
	Follower robot 1	x	y	44.6
		8.2	8.2	
	Follower robot 2	x	y	
		6.8	6.8	
	Follower robot 3	x	y	
		6.8	6.8	

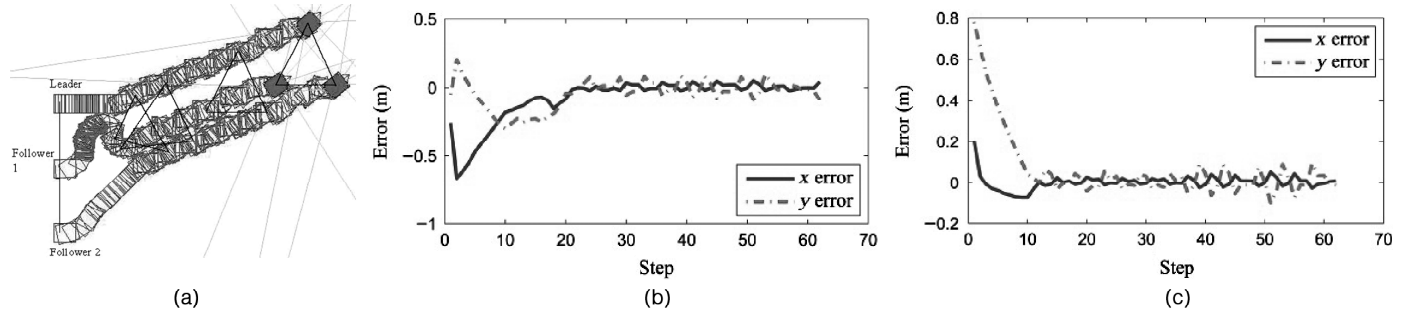

Figure 5. Formation switching in MobileSim simulator: (a) trajectories; (b) position errors of follower 1; and (c) position errors of follower 2.

6.1 Formation Switching

The experiment validates that the exchange between two different formations successfully achieves with the proposed algorithm in MobileSim simulator. The desired formation shape is an equilateral triangle, and the desired separation distance equals 1 m.

Figure 5 shows several results where three robots switch between two different shapes. From these figures, we note that follower robots quickly track the leader robot.

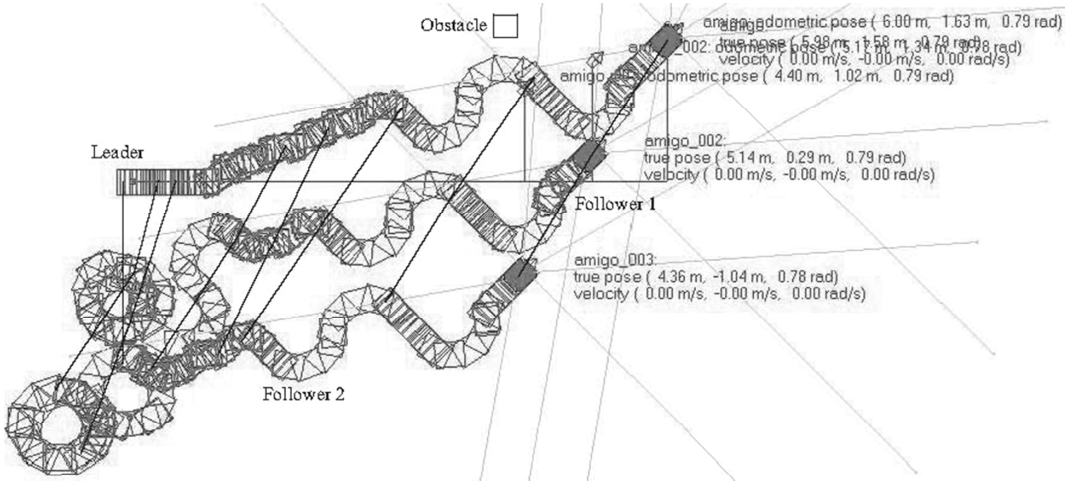

Figure 6. Formation with obstacle avoidance in MobileSim simulator.

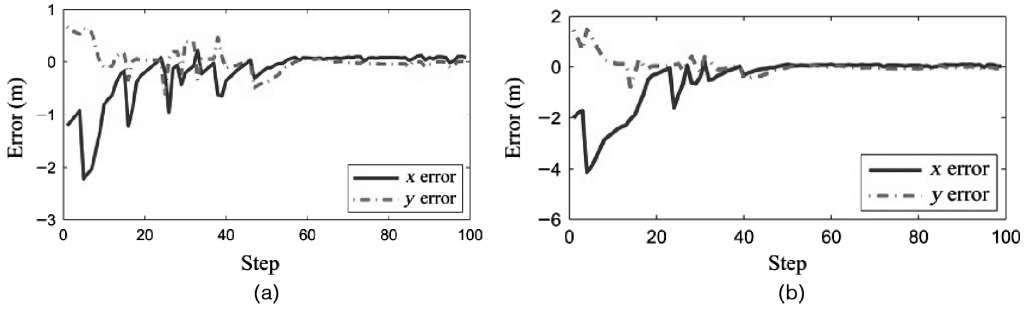

Figure 7. Position errors of follower robots: (a) position errors of follower 1; (b) position errors of follower 2.

6.2 Formation with Obstacle Avoidance

The experiment proves that the proposed algorithm forms the desired formation with obstacle avoidance in MobileSim simulator. The position of the obstacle is specified as (4,2) m. The desired separation distance equals 1.5 m, and the desired bearing angle equals $\pi/3$.

Figure 6 shows the formation trajectories of multi-robot systems with obstacle avoidance. Figure 7(a) and 7(b) show the position errors of follower robots 1 and 2. From these figures, we can note that multi-robot systems successfully avoid the obstacle and form the desired formation. Position errors of follower robots converge to zeros quickly.

7. Conclusion

The proposed algorithm combining artificial immune network and position tracking control method successfully achieves formation with obstacle avoidance. The steering direction and the linear velocity for follower robot are computed with different algorithms. The steering direction of follower robot is calculated with AINA. Follower robot selects the optimal steering direction in many possible directions based on the steering direction of leader robot, the azimuth of virtual robot, and the distance from obstacle. The optimal steering direction quickly tends towards the steering direction of leader robot, and successfully avoids obstacles. The linear velocity of follower robot is calculated with position tracking control method. It guarantees that the state errors of follower robots converge to zeros quickly. The asymptotic stability of the entire formation system is proven with Lyapunov theory. Several Matlab simulations and MobileSim experiments validate that the proposed algorithm successfully avoids obstacles and quickly recovers formation after passing around obstacles.

Acknowledgement

This work was supported in part by the National High Technology Research and Development Program 863, China (2015AA042307), Shandong Provincial Independent Innovation & Achievement Transformation Special Foundation, China (2014ZZCX04302, 2014ZZCX04303), Shandong Provincial Scientific and Technological Development Foundation, China (2014GGX103038), and the Fundamental Research Funds of Shandong University (2015JC027, 2015JC051).

References

[1] J. Ni, X. Yang, J. Cheng, and S.X. Yang, Dynamic bioinspired neural network for multi-robot formation control in unknown environments, *International Journal of Robotics and Automation*, *30*(3), 2015, 206–4217.

[2] G. Rishwaraj, S.G. Ponnambalam, and R.M. Kuppan Chetty, Multi-robot formation control using a hybrid posture estimation strategy, *International Journal of Robotics and Automation*, *29*(4), 2014, 206–4078.

[3] Y.-T. Wang and Y.-C. Chen, Multiple-obstacle avoidance in role assignment of formation control, *International Journal of Robotics and Automation*, *27*(2), 2012, 206–3430.

[4] A. Noormohammadi Asl, M.B. Menhaj, and A. Sajedin, Control of leader-follower formation and path planning of mobile robots using Asexual Reproduction Optimization (ARO), *Applied Soft Computing*, *14*, 2014, 563–576.

[5] L. Consolini, F. Morbidi, D. Prattichizzo, and M. Tosques, Leader-follower formation control of nonholonomic mobile robots with input constraints, *Automatica*, *44*(5), 2008, 1343–1349.

[6] Debabrata Atta and Bidyadhar Subudhi, Decentralized formation control of multiple autonomous underwater vehicles, *International Journal of Robotics and Automation*, *28*(4), 2013, 206–3613.

[7] L. Yang, Z. Cao, and M. Tan, Dynamic formation control for multiple robots in uncertain environments, *Robot*, *32*(2), 2010, 283–288.

[8] R. K. Chetty, M. Singaperumal, and T. Nagarajan, Distributed formation planning and navigation framework for wheeled mobile robots, *Journal of Applied Sciences*, *11*(9), 2011, 1501–1509.

[9] Y. Dai, and S.-G. Lee, The leader-follower formation control of nonholonomic mobile robots, *International Journal of Control, Automation and Systems*, *10*(2), 2012, 350–361.

[10] T.-T. Yang, Z.-Y. Liu, H. Chen, and R. Pei, Formation control and obstacle avoidance for multiple mobile robots, *Acta Automatica Sinica*, *34*(5), 2008, 588–593.

[11] T. Zhang, X. Li, Y. Zhu, and S. Chen, *et al.*, Formation and obstacle avoidance in the unknown environment of multi-robot system, *Proceedings of the IEEE International Conference on Robotics and Biomimetics*, 2009, 729–734.

[12] J.V. Gomez, A. Lumbier, S. Garrido, and L. Moreno, Planning robot formations with fast marching square including uncertainty conditions, *Robotics and Autonomous Systems*, *61*, 2012, 137–152.

[13] S. Liu, D. Sun, and C. Zhu, A dynamic priority based path planning for cooperation of multiple mobile robots in formation forming, *Robotics and Computer-Integrated Manufacturing*, *30*(6), 2014, 589–596.

[14] Y. Dai and S.-G. Lee, Formation control of mobile robots with obstacle avoidance based on GOACM using onboard sensors, *International Journal of Control, Automation, and Systems*, *12*(5), 2014, 1077–1089.

[15] G.-C. Luh and W. Liu, An immunological approach to mobile robot reactive navigation, *Applied Soft Computing*, *8*(1), 2008, 30–45.

[16] L. Deng, X. Ma, J. Gu, and Y. Li, Mobile robot path planning using polyclonal-based artificial immune network, *Journal of Control Science and Engineering, 2013*, 2013, 1–13.

[17] L. Deng, X. Ma, J. Gu, and Y. Li, Planning multi-robot formation with improved poly-clonal artificial immune algorithm, *International Conference on Robotics and Biomimetics*, 2013, 982–987.

[18] L. Deng, X. Ma, J. Gu, and Y. Li, Multi-robot dynamic Formation path planning with improved polyclobal artificial immune algorithm, *Control and Intelligent Systems*, *4*(42), 2014, 1–8.

[19] L. Deng, X. Ma, J. Gu, and Y. Li, Improved poly-clonal artificial immune network for multi-robot dynamic path planning, *International Conference on Information and Automation*, 2013, 128–133.

[20] Y.-Y. Min and Y.-G. Liu, Barbalat Lemma and its application in analysis of system stability [J], *Journal of Shandong University (engineering science)*, *1*(1), 2007, 1–6.

Biographies

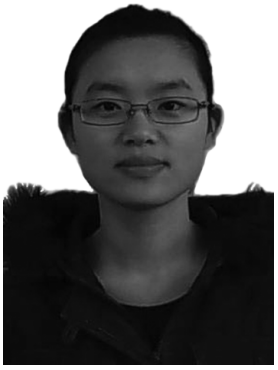

Lixia Deng received her bachelor's degree in Electrical Engineering and Automation from Shandong Jiaotong University, China in 2011. Since then, she is a graduate student and doctoral student in School of Control Science and Engineering, Shandong University, China. Her research interests mainly include artificial immune algorithm, multiple mobile robots dynamic path planning, and multi-robot formation. She is a student member of IEEE.

Xin Ma received her B.S. degree in industrial automation and M.S. degree in automation from Shandong Polytech University, China in June 1991 and June 1994. She received her Ph.D. degree in aircraft control, guidance, and simulation from Nanjing University of Aeronautics and Astronautics, China in June 1998. She is a professor at Shandong University. Her current research interests include mobile sensor network, multiple mobile robots, and machine vision. Dr. Ma is a member of IEEE.

Jason Gu received his B.S. degree in Electrical Engineering and Information (Special Class for the Young Gifted, 1987–1990) from the University of Science and Technology of China, China in 1992. He received his M.Sc. degree in Biomedical & Instrumentation Engineering from Shanghai Jiaotong University, China in 1995. He earned his Ph.D. degree from the Department of Electrical and Computer Engineering, University of Alberta, Canada in 2001. From 2009, he has been a full professor in Dalhousie University, Canada. His research interests include robotics, biomedical engineering, control systems, and intelligent systems. Dr. Gu is a senior member of IEEE and Fellow of Engineering Institute of Canada.

Yibin Li received his B.S. degree in Automation from Tianjin University, China in 1982, his M.S. degree in Electrical Automation from Shandong University of Science and Technology, China in 1990, and his Ph.D. degree in Automation from Tianjin University in 2008. From 1982 to 2003, he worked at the Shandong University of Science and Technology, China. Since 2003, he has been

the Director of Center for Robotics, Shandong University. His research interests include bionic robots, control of intelligent robots, machine learning, and intelligence architecture.

Zhigang Xu received his B.S. degree in Biochemistry from Yantai University in 1998, and Ph.D. degree in Genetics from Fudan University in 2004. He then did his postdoctoral research in Harvard Medical School and Stanford University School of Medicine from 2005 to 2009, and is currently a professor in Shandong University School of Life Sciences. His research interests include hearing transduction, hearing loss, and auditory protection. He is a member of ARO, SfN and CSCB.

Yafang Wang obtained her B.S. and M.S. degrees at School of Computer Science and Technology at Shandong University in 2006 and 2009, respectively. From September 2007 to September 2008, she attended the Double Master Degree Program in Computer Science between University of Luxembourg and Shandong University, and her major was Security and Trust. She received a Ph.D. degree in Database and Information Systems group at Max Planck Institute for Informatics, Germany, in February 2013, and worked as a postdoctoral researcher in the same group from March 2013 until September 2013. Her supervisor is Prof. Gerhard Weikum. Since October 2013, she has been working as an associate professor at the School of Computer Science and Technology, Shandong University. Her research interests include knowledge harvesting, semantic analytics, and multimedia knowledge bases.